

# A Linear Flow Channel Reactor for High Sulphate Water Treatment: A Simple and Practicable AMD Treatment System for Rural Communities in South Africa

JB Witbooi<sup>1</sup>, IG Mkhize<sup>2\*</sup>, FB Waanders<sup>1</sup>, AC Eloka-Eboka<sup>1</sup>, SKO Ntwampe<sup>2</sup>

<sup>1</sup>*School of Chemical and Mineral Engineering, Faculty of Engineering and the Built Environment, North-West University, Potchefstroom, 2531, South Africa, witbooijan40@gmail.com, Frans.Waanders@nwu.ac.za, fadafounder@gmail.com*

<sup>2</sup>*Department of Chemical Engineering, Faculty of Engineering and the Built Environment, Durban University of Technology, Durban, 4001, South Africa, InnocentiaM2@dut.ac.za, SetenoN@dut.ac.za*

## Abstract

AMD remains a major challenge posed by both abandoned and active mines. A 12 L LFCR was operated for 110 d using a floating sulphur biofilm (FSB) supported by ethanol. Across Periods I (40 d), II (30 d), and III (40 d), sulphate and COD removal reached 99%, 92%, and 94%, and 95%, 77%, and 78%, respectively. Sulphide production was 195, 144, and 233 mg L<sup>-1</sup>. Fe, Cu, Ni, and Zn removal exceeded 95% within days, with Mn reduced over longer operation, while pH stabilised at 6.8-7.5. A feed-forward network predicted sulphate removal ( $R^2 = 0.75$ ), with overall strong reactor stability.

**Keywords:** Acid mine drainage, biological sulphate reduction, sulphate-reducing bacteria, linear flow channel reactor, hydraulic retention time, feed forward network

## Introduction

One of the threats to freshwater resources is acid mine drainage (AMD) (Baloyi *et al.* 2024). In South Africa (SA), AMD is generated by the mineral production industry, primarily through mining. AMD is produced by the oxidation of sulphide-rich gangue and coal deposits. Specific environmental problems, such as high sulphate concentrations, elevated dissolved metal concentrations, and low pH, are associated with AMD. Biological sulphate reduction (BSR) (Mafane *et al.* 2025) is a process that employs sulphate-reducing bacteria (SRB) to treat AMD by removing sulphate and metal contaminants and producing sulphide.

A linear flow channel reactor (LFCR) (Marais *et al.* 2022b) capable of integrating both the biological sulphate reduction (BSR) process and partial sulphide oxidation, can treat AMD. The reactor demonstrated satisfactory performance in removing sulphates from AMD and can handle the more toxic sulphide by developing a floating sulphur biofilm (FSB). Furthermore, the LFCR presents a practical, low-cost, and low-energy solution for rural communities

affected by AMD. Its simple design and minimal operational requirements make it ideal for areas with limited technical capacity, while still achieving high removal efficiency for sulphate and metal contaminants. Importantly, the FSB enables safe sulphide management and supports potential recovery of elemental sulphur (S<sup>0</sup>) (Marais *et al.*, 2022a), offering circular-economy opportunities for agriculture-based livelihoods. By relying on naturally occurring microbial processes and inexpensive organic carbon sources, the LFCR provides a sustainable alternative to chemically intensive and energy-dependent AMD remediation operations. Implementing such systems in rural communities can protect freshwater resources, improve public health, and stimulate community-level economic value from AMD streams.

## Methods

An LFCR with total volume 12 L, operational volume 9 L, dimensions 800 mm × 100 mm × 150 mm, 11 mm thick Perspex, and 15 sampling ports was used – see Fig. 1. AMD (Quality characteristics are listed in Table 1) was supplied in 25 L containers by the Council

for Mineral Technology (Randburg, Gauteng province, South Africa), hereafter referred to as Mintek. Ethanol was used as a sole carbon source. The reactor was operated for 110 d, divided into Period I (40 d), Period II (30 d), and Period III (40 d).

### *LFCR Sampling, Monitoring, Process Control, and Operational Adjustments*

The operation of the LFCR followed a structured strategy designed to sustain BSR, maintain a stable FSB, and ensure robust performance under varying feed conditions over time. The reactor influent comprised a controlled mixture of AMD and an SRB-rich inoculum supplied by Mintek (developed as reported elsewhere by Preez and Marumo, 2024), together with a fixed ethanol dose as the electron donor (Table 1). To stabilize biological activity and interrogate system resilience, the AMD-to-inoculum ratio was deliberately varied across three operating periods: during Period I, a high inoculum fraction promoted rapid SRB acclimation and strong early sulphate reduction; in Period II, an increased AMD load and reduced inoculum concentration spiked Mn imposed more acidic and metal-rich conditions to stress the system; and in Period III, the inoculum fraction was increased to facilitate performance recovery following the stressed regime, Period II. Ethanol was supplied at a constant dosage throughout all periods to

ensure a consistent carbon source irrespective of feed composition. Sampling ports ( $n=15$ ) were distributed along the reactor length, with nine central ports routinely used to avoid zones affected by surface biofilm formation or bottom sediment accumulation. Sampling was conducted daily by withdrawing 30 mL of reactor fluid into 50 mL tubes for analysis of pH, sulphate, sulphide, COD, and dissolved metals, with rubber septa replaced regularly to prevent leakage and preserve anaerobic conditions. Over the 110-day operational campaign, intentional step changes in feed composition and hydraulic retention time were applied to evaluate system resilience, inducing stress during Period II and enabling recovery during Period III. In parallel, routine visual inspection of the biofilm, assessing colour, thickness, and structural integrity, provided qualitative insight into sulphide oxidation behaviour and potential oxygen ingress.

### *Reactor Loading and Hydraulic Retention Time*

The LFCR was filled using a low-flow peristaltic pump operating at a fixed rate, thereby providing the desired hydraulic residence time (HRT). The operational plan deliberately shifted the HRT across periods: 3 d in Periods I and III, 2 d in Period II. These changes were used to examine how reduced contact time affects SRB performance and

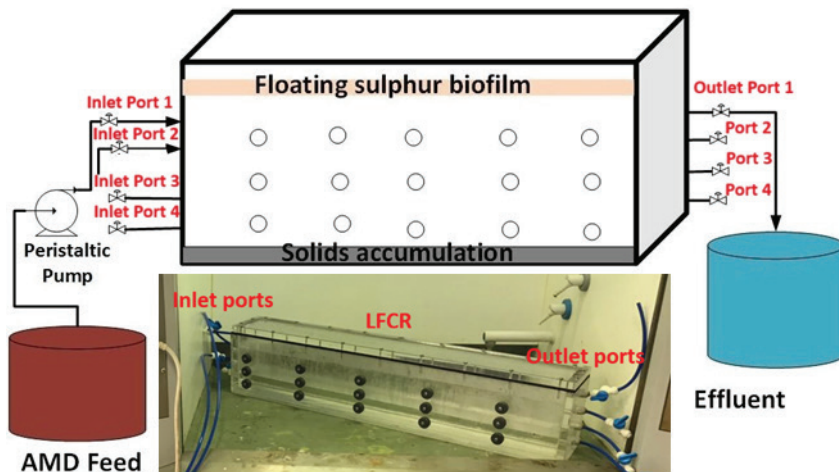


Figure 1 The complete LFCR design and operation setup.



sulphate-reduction efficiency. The reactor remained closed to mixing, allowing the LFCR's characteristic laminar-like, stratified flow regime to develop. This flow pattern was essential for maintaining anaerobic conditions within the biofilm while sustaining a microoxic zone at the liquid-biofilm interface.

### *Establishment and Management of the Floating Sulphur Biofilm*

Once the reactor was filled, it was left unoperated for 2 to 3 d to allow the FSB to form at the air-AMD interface. As the operation continued, the biofilm thickened progressively as SRB biofilm became established (see Figure 2). The FSB served dual roles: (i) restricting oxygen transfer into the bulk liquid and enabling potential partial oxidation of sulphide to S<sub>0</sub>, which subsequently accumulated in the biofilm. Later in the run (Period III), signs of biofilm ageing and structural weakening, i.e., sloughing, appeared, indicating the need for periodic harvesting or maintenance in long-term operation. Maintaining the integrity of this biofilm was central to the reactor operation strategy.

### *Feed Forward Network Methodology*

The feed-forward network (FFN) was used to predict effluent sulphide concentration from routinely measured process variables, with effluent sulphide as the dependent variable

and influent COD, bulk pH, and sulphate concentration as inputs. The full dataset collected over the 110-day campaign was cleaned to remove outliers, normalised, and partitioned into training (70%) and testing (30%) subsets to enable validation and avoid overly optimistic performance estimates. The FFN had a single hidden layer (3 neurons) and a linear output. As in Fig. 3, the hidden units used tan-sig (hyperbolic tangent) activation, while the output layer used purelin (linear).

Training employed the Levenberg-Marquardt optimisation, chosen for its fast convergence in small - to medium-sized regression problems. Implementation was done in MATLAB (R2020a). To benchmark non-linear learning against a simpler alternative, a multiple linear regression (MLR) model using the same inputs was also developed. Model validity was assessed using R<sup>2</sup>, RMSE, and MAE on both training and test partitions.

### *Routine Analyses*

The pH of the influent, reactor samples, and effluent was measured using a calibrated glass electrode on a Metrohm 744 pH meter. The 10 mL samples were filtered and sent for analysis using Thermo Fisher Scientific's 6200 inductively coupled plasma optical emission spectrometry (ICP-OES) to determine the presence of, amongst others, Mn, Fe, Ni, Cu, and Zn. COD was measured using a HI83399 Hanna multiparameter photometer.

**Table 1** Operating conditions for the three periods during which the LFCR was in operation.

Parameter	Period I	Period II	Period III
AMD volume (L)	6	7	5
Inoculum volume	2	1	3
Ethanol volume (mL)	30	30	30
Reactor liquid volume (L)	9	9	9
Oxygen requirement	Anaerobic	Anaerobic	Anaerobic
Influent pH	5.84	5.13	5.72
Influent sulphide concentration (mg L <sup>-1</sup> )	55	41	3.4
Influent sulphate concentration (mg L <sup>-1</sup> )	4179	5050	2761
Temperature (°C)	25	25	25
Hydraulic residence time (HRT) (d)	3	2	3
Sulphate:COD ratio	0.7	0.9	0.6

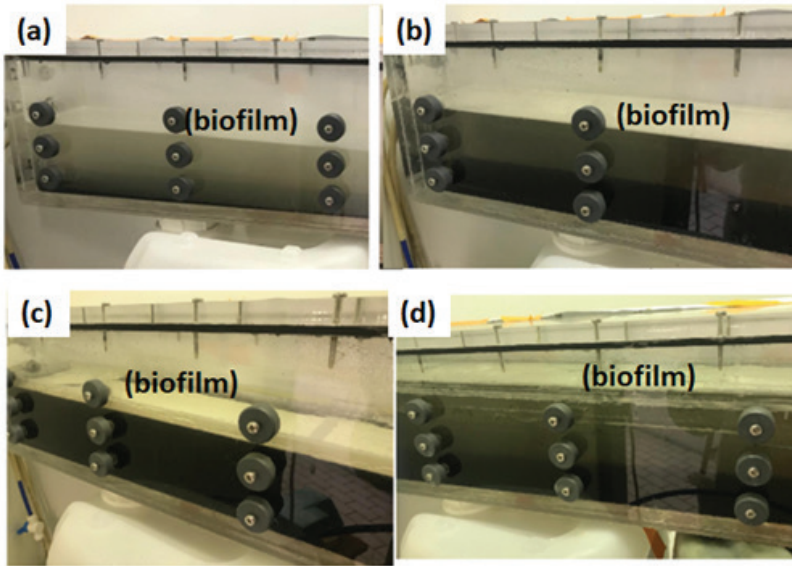


Figure 2 Formation and maturing of the biofilm throughout the reactor operation, at (a), 3, (b) 40, (c) 70 (c) and (d) 90 d.

The sulphides present in the samples were measured using the Methylene Blue method. The sulphate content in the samples was measured using a Shimadzu UVmini-1240 UV spectrophotometer.

## Results

### LFCR Performance Analysis

The LFCR's performance indicators, sulphate removal, COD reduction, dissolved metal contaminants, and sulphide production, showed robust but period-dependent performance. Sulphate removal reached 99% in Period I, decreased to 92% in Period II, and recovered to 94% in Period III, while COD reduction declined from 95% to 77–78% under stressed conditions. Peak sulphide concentrations (195, 144, and 232 mg L<sup>-1</sup>, respectively) reflected biological activity coupled with oxidation and precipitation (Baloyi *et al.* 2023; Horn *et al.* 2022). These trends are consistent with expectations that reduced HRT and elevated sulphate:COD ratios suppress sulphidogenesis, whereas sufficient HRT and carbon availability restore performance. Reactor pH rapidly stabilised near neutral during Period I ( $\approx 7.0$ – $7.5$ ) due to alkalinity

generation during BSR, declined and became more variable in Period II ( $\approx 6.0$ – $6.5$ ) under increased acid loading, and recovered to 6.8–7.0 in Period III, although late-stage biofilm ageing was evident. Metal contaminants removal exhibited a two-timescale response: (i) rapid attenuation of Fe, Cu, Ni, and Zn to near-nondetectable levels within 10–15 days, a response seen elsewhere (Baloyi *et al.* 2024), (ii) followed by slower Mn removal governed by its stronger pH dependence (Smičiklas *et al.* 2023). A transient Mn increase following the addition of fresh AMD (30–37 days) was subsequently stabilised at  $\approx 2.8$  mg L<sup>-1</sup> as the SRB community acclimated, consistent with

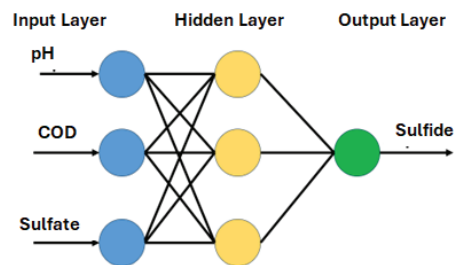


Figure 3 The FFN model structure used for modelling.



**Table 2** Period-wise pH stabilisation and trace metal removal.

Period (d)	pH stabilisation	Performance evaluation
I (1–40)	Stabilised around pH 7.0–7.5 as SRB adapted.	Ni, Cu, Zn: $\approx 0.9 \text{ mg L}^{-1}$ initially to nondetectable by 15 d. Fe: $\approx 37 \text{ mg L}^{-1}$ to $\approx 1 \text{ mg L}^{-1}$ by 10 d. Mn: fell from $\approx 12 \text{ mg L}^{-1}$ ; extended tracking reached $\approx 0.1 \text{ mg L}^{-1}$ by 30 d, then later fluctuated (Period II).
II (41–70)	Fluctuated around pH 6.0–6.5 with higher AMD load and lower inoculum.	Mn: after reaching $\approx 0.1 \text{ mg L}^{-1}$ by 30 d, spiked to $\approx 12 \text{ mg L}^{-1}$ with new AMD addition (30–37 d), then declined to $\approx 2.8 \text{ mg L}^{-1}$ as SRB re-adapted.
III (71–110)	Stabilised around pH 6.8–7.0 with higher inoculum; some biofilm ageing noted late	Overall, sulphate and COD removal performance remained high and consistent with Period I and II trends.

the known requirement for higher pH and longer HRT for effective Mn removal (Zhao *et al.* 2024). A summarised performance evaluation is listed in Table 2.

Overall, alkalinity generation moderates influent acidity, thereby promoting metal sulphide precipitation and the rapid removal of Fe, Cu, Ni, and Zn. The transient Mn increase following the addition of fresh AMD reflects an acid-metal pollutant shock, followed by stabilisation as pH and sulphide speciation recover and the FSB's buffering role takes effect. From a process-control perspective, the period-wise data reinforce established LFCR behaviour, (i) reducing HRT from 3 to 2 days curtailed contact time and carbon utilisation, lowering sulphate and COD removal, whereas restoring HRT improved performance. Increasing the sulphate-to-carbon ratio constrained SRB activity and sulphide production, while lowering it relieved carbon limitation. Increasing the inoculum fraction in Period III restored near-neutral pH and sulphate removal, offsetting the mid-campaign decline.

Several features distinguish this study and strengthen the case for decentralized rural AMD treatment: (i) integration of BSR and partial sulphide oxidation in a single unit enables sulphide control without downstream reactors, reducing energy and chemical inputs while possibly generating recoverable elemental sulphur; (ii) semi-passive open-channel operation minimizes mechanical requirements, easing operation where power and skilled labour are limited; (iii) effective metal pollutant

removal, combined with near-neutral pH, demonstrates that compact LFCRs can achieve regulatory-relevant discharge water requirements under realistic feed conditions; and (iv) ethanol, with potential substitution by low-cost local organics, provides flexibility in carbon sourcing. The constraint associated with biofilm ageing late in Period III indicates the need for maintenance, such as periodic FSB harvesting.

#### *Long Term Performance: Operational Sustainability*

While the LFCR demonstrated sustained sulphate and metal removal over 110 days, the late Period III performance decline highlights long-term sustainability challenges associated with biofilm ageing and excess sulphur accumulation, which impair mass transfer and sulphide oxidation. Stable long-term operation can be achieved through conservative loading conditions, routine monitoring, and simple biofilm management such as periodic manual harvesting, consistent with the system's semi-passive, low-energy design. Operational stressors, including reduced hydraulic residence time and high sulphate-to-COD ratios, were shown to accelerate performance loss via carbon limitation and microbial stress. Crucially, performance recovery after reinoculation and restoration of HRT demonstrated LFCR resilience, supporting their suitability for decentralised AMD treatment and confirming that biofilm ageing is a manageable maintenance issue rather than a fundamental limitation



### Feed-Forward Network Performance.

BSR-FNN integrates microbially mediated redox reactions, alkalinity generation, sulphide production and oxidation, and metal precipitation, all of which respond non-linearly to pH, electron-donor availability, and chemical speciation (Yao *et al.* 2024). Because FFNs learn non-linear input-output relationships, the FFN captured interactions that linear regression could not, yielding higher test-set  $R^2$  values and lower error metrics (Karadurmuş *et al.* 2024). The choice of COD, pH, and sulphide as predictors was physically justified: COD represents electron-donor supply to the SRB, pH governs microbial activity and precipitation equilibria, and sulphide is both a BSR/LFCR product and a reactant in partial oxidation and metal sulphide formation. The compact FFN architecture (one hidden layer with three neurons) achieved a practical bias–variance trade-off, remaining sufficiently expressive to model the non-linear behaviour of the LFCR while limiting overfitting for the available dataset. Model performance was FFN:  $R^2$  (train/test) = 0.93/0.75, RMSE = 389/483 mg L<sup>-1</sup>, MAE = 228/305 mg L<sup>-1</sup>; and MLR:  $R^2$  = 0.83/0.42, RMSE = 589/735 mg L<sup>-1</sup>, MAE = 425/541 mg L<sup>-1</sup>, confirming substantially better generalisation by the FFN, consistent with the inherent non-linearity of sulphidogenic systems.

The residual train-test gap indicated potential for improvement through the inclusion of additional process variables (e.g., HRT, sulphate: COD ratio, inoculum fraction, temperature), expansion of the dataset across additional operating regimes, or the use of regularisation strategies. The superior FFN performance aligns with prior wastewater and bioprocess modelling studies, where neural networks outperform linear models for variables governed by multi-factor kinetics. In LFCRs, where sulphate reduction beneath the FSB is coupled with potential partial sulphide oxidation at the interface, real-time sulphate soft sensing could help identify carbon limitation, detect acid or metal shocks, and schedule FSB maintenance to prevent LFCRs' underperformance. While

the present dataset spans a single 110-day campaign with three operating periods, broader generalizability would benefit from additional campaigns covering wider ranges of HRT, sulphate/COD ratio, temperature, and inoculum conditions.

### Conclusions

The campaign showcases a compact, low-energy LFCR that can stably neutralise pH, achieve high sulphide and COD removal, and rapidly clear metals (with Mn requiring additional residence time and pH control), all while converting sulphide to elemental sulphur within the reactor. The data are consistent with recent LFCR literature on HRT sensitivity, FSB-mediated sulphur recovery, and microbial adaptation across reactor zones, consolidating the case for semi-passive, circular-economy AMD treatment in resource-constrained settings. Lastly, FNN outperformed linear regression, achieving better generalisation to unseen data (test  $R^2$   $\approx$  0.75 with lower RMSE/MAE) and thus is the preferred model for predicting effluent sulphate concentration in the LFCR.

### Acknowledgements

I am grateful to my supervisors, laboratory staff, technical colleagues, and my family for their continuous guidance, assistance, and encouragement throughout this research journey. I also thank North-West University and Sasol for the financial support that made the successful completion of this study possible.

### Declaration

The research reported herein was the subject of a master's thesis at the North-West University, South Africa, in 2025.

### References

- Baloyi J, Ramdhani N, Mbhele R, Simate GS (2024) Acid mine drainage from gold mining in South Africa: Remediation, reuse, and resource recovery. *Mine Water and the Environment* 43:418–430.
- Baloyi J, Ramdhani N, Mbhele R, Ramutshatsha-Makhwedzha D (2023) Recent progress on acid mine drainage technological trends in South Africa: Prevention, treatment, and resource recovery. *Water* 15(19):3453.
- Marais TS, Huddy RJ, Harrison STL (2022a) Elemental sulphur recovery from a sulphate-rich aqueous stream in a single hybrid linear flow channel reactor



- is mediated through microbial community dynamics and adaptation to reactor zones. *FEMS Microbiology Ecology* 98:fiac059.
- Marais TS, Huddy RJ, Van Hille RP, Harrison STL (2022b) Effect of temperature change on the performance of the hybrid linear flow channel reactor and its implications on sulphate-reducing and sulphide-oxidising microbial community dynamics. *Frontiers in Bioengineering and Biotechnology* 10:908463.
- Horn EJ, van Hille RP, Oyekola OO, Welz PJ (2022) Functional microbial communities in hybrid linear flow channel reactors for desulfurization of tannery effluent. *Microorganisms* 10(11):2305.
- Mafane D, Ngulube T, Mphahlele-Makgwane MM (2025) Anaerobic bioremediation of acid mine drainage using sulphate-reducing bacteria: Current status, challenges, and future directions. *Sustainability* 17(8):3567.
- Smičiklas I, Janković B, Jović M, Maletaškić J, Manić N, Dragović S (2023) Performance assessment of wood ash and bone char for manganese treatment in acid mine drainage. *Metals* 13(10):1665.
- Yao Y, Li Y, Shi Y, Shi K, Bai Y, Gao Y, Jiang Q, Xue J, Cheng D (2024) Prediction of artificial neural network for sulfate removal from wastewater and analysis of key factors in an anaerobic biological system. *Journal of Environmental Chemical Engineering* 12:112085.
- Karadurmuş E, Göz E, Keleş C, Yüceer M (2024) Utilizing artificial neural networks (ANN) for predictive modeling of sulfate removal from water. *Sigma Journal of Engineering and Natural Sciences* 42(6):1866–1875.
- Preez, K. D., Marumo, M. (2024). Feasibility of the scale-up of a semi-passive biological sulfate reduction process treating high sulfate mine-influenced water. In West Virginia Mine Drainage Task Force Symposium, International Mine Water Association Congress: Morgantown, VA, USA.
- Zhao P, Zhang R, Hu M (2024) Alkaline chemical neutralization to treat acid mine drainage with high concentrations of iron and manganese. *Water* 16(6):821.